

UNITED STATES
DEPARTMENT OF THE INTERIOR
GEOLOGICAL SURVEY

GENERAL CHARACTERISTICS AND AVAILABILITY OF LANDSAT 3
AND HEAT CAPACITY MAPPING MISSION THERMAL INFRARED DATA

By C. Scott Southworth

Open-File Report 83-123

Reston, Virginia

May 1983

General Characteristics and Availability of Landsat 3
and Heat Capacity Mapping Mission Thermal Infrared Data

by

C. Scott Southworth
U.S. Geological Survey
Reston, Va. 22092

Abstract

Two satellite systems launched by the National Aeronautics and Space Administration (NASA) in 1978 carried sensors which operated in the thermal infrared (IR) region of the electromagnetic spectrum. Thermal IR radiation data provide spectral information about the physical properties of the Earth's surficial materials not duplicated in either the visible or reflective IR wavelength regions. Landsat 3, launched on March 5, 1978, contained a thermal sensor as part of the multispectral scanner (MSS) system. The sensor operated in the 10.4- to 12.6- μm (band 8) wavelength region and produced imagery with a ground resolution of approximately 238 m.

Launched on April 26, 1978, the Heat Capacity Mapping Mission (HCMM) spacecraft carried a sensor, the heat capacity mapping radiometer (HCRM) which operated in the 10.5- to 12.5- μm wavelength region and produced imagery with a ground resolution of approximately 600 m at nadir. The HCMM satellite acquired over 6,600 data passes of visible (0.55-1.1 μm), as well as thermal IR data, over North America, Europe, and Australia.

General characteristics and availability of Landsat 3 and HCMM thermal IR data are discussed. Landsat 3 reflected IR band 7 (0.8-1.1 μm) and Landsat 3 band 8 thermal data acquired over the eastern and western United States are analyzed and compared with HCMM visible, thermal IR, thermal inertia, and day-night temperature difference imagery for geologic applications. Digitally processed and enhanced HCMM data (high-pass filters, diagonal derivatives, and band ratios), produced by the U.S. Geological Survey, Flagstaff, Ariz., are presented for geologic interpretation.

INTRODUCTION

Prior to 1978, the primary method of thermal data acquisition was either by aircraft or meteorological satellite. Aircraft acquired thermal scanner data are restricted in geographic coverage and costly, while meteorological satellites, such as NOAA's, are of too low spatial and thermal resolution to be useful for most geologic purposes. Two satellite systems launched by NASA in 1978 carried sensors which operated in the thermal IR region of the electromagnetic spectrum. Landsat 3, launched on March 5, 1978, contained, as part of the multispectral scanner (MSS) system, a thermal sensor which operated in the 10.4- to 12.6- μm wavelength region. Launched on April 26, 1978, the Heat Capacity Mapping Mission (HCMM) spacecraft carried a special thermal sensor, the heat capacity mapping radiometer (HCMR) which operated in the 0.55- to 1.1- μm and 10.5- to 12.5- μm wavelength region.

There are two principal atmospheric windows in the thermal infrared region, 3.0-5.0 μm and 8.0-14.0 μm . The 8.0-14.0- μm window passes the maximum intensity of the Earth's radiant energy flux and is preferred to the 3- to 5- μm atmospheric window (Sabins, 1978).

Thermal IR radiation data complement surface reflectance data in providing information about the physical properties of the Earth's surficial material. Thermal IR data allow discrimination of materials which have similar reflectance values but different thermal properties (for example, limestone vs. dolomite). Thermal inertia, a property derived from the ability of a material to conduct heat into and out of its bulk, is dependent on density, moisture content, and composition of materials, and thus, is an important tool for geologic mapping.

Variations in image gray scales and computer tape numerical values represent different radiometric emittance from the Earth's surface. Manual interpretation provides information on topography and geology not produced from the visible to near infrared regions. As with Landsat data, optimal analysis requires digital computer processing.

The geologic remote sensing community should be familiar with the existing satellite-acquired thermal data to accurately assess the thermal data from the thematic mapper (TM). Carried on Landsat 4, the TM band 6 obtains thermal data in the 10.5- to 12.5- μm waveband region with an increased spatial resolution to previous satellite acquired thermal data.

Landsat 3 - Band 8

The thermal sensor on Landsat 3 operated in the 10.4- to 12.6- μm wavelength region, band 8, and has a ground resolution of approximately 238 m. Table 1 gives the general characteristics of band 8. The Landsat 3 band 8 sensor consisted of two mercury-cadmium-telluride thermal infrared detectors having a range of thermal detection from 260^o to 340^o K. The band 8 fiber optics at the focal plane of the MSS is three times the size of the fiber optics of bands 4 through 7, which gives band 8 ground instantaneous field of view (IFOV) of 238 meters square at nominal altitude (920 km or 570 miles). The spatial resolution of 238 m gives a sampling rate of 1/9 that of the 79-m-resolution MSS band 4 through 7 data.

The Landsat 3 band 8 sensor malfunctioned producing coarse spatial and thermal resolution. After the first outgassing cycle for the cooling of the thermal detector in mid-March 1978, the thermal resolution of Landsat 3 band 8 was approximately 1.2° K, better than the 1.5° K resolution of pre-flight specifications (Lougeay, 1981). Rapid outgassing from within the instrument for the cooling of the thermal detector formed condensation on the detector window with a resultant loss of detector sensitivity. The decrease in detector output voltage, corrected by a compensating increase in the gains of the preamplifier, decreased the signal-to-noise ratio (Price, 1981). Striping of the data resulted due to the differing performance of detectors (along track) and change in detector sensitivity (across track) (Price, 1981). Although the thermal sensor frequently malfunctioned and became inoperative in early 1979, over 370 thermal IR images were acquired during the day descending node and over 50 scenes were acquired during the night ascending node, over the conterminous United States during the initial 4-month period of operation. Low spatial resolution, low thermal sensitivity ($\pm 1.50^{\circ}$ K), and high noise level allow some qualitative analysis but no quantitative analysis of the data.

Landsat data are archived and distributed to the public by the EROS Data Center, Sioux Falls, South Dakota. Landsat 3 band 8 data can be accessed through two means: (1) microfiche indexes containing day acquired data, and (2) INORAC (Inquiry Orders and Accounting) computer system containing day and night acquired data (U.S. Geological Survey, 1979).

On microfiche indexes, the band 8 designator column contains an asterisk (*) if no data were acquired or a number ranging from 0 to 8 (very poor to good) to indicate quality of acquired data. No band 8 data are contained on 16-mm microfilm for viewing. In the INORAC system, Landsat 3 thermal data acquired during the day may be accessed by world reference system path and row by specifying the Landsat 3 satellite (SA:3) and band 8 sensor (SO:AE). Band 8 data acquired at night are accessible by specifying recording technique (RE:39). Because of the ascending orbit, path/row numbers do not correspond to those on the descending node, so searches are entered by geographic coordinates. Landsat 3 band 8 data, acquired simultaneously with bands 4-7 data during the day, may be recorded on high-density tapes or 9-track 1,600-bpi computer-compatible tapes (CCT) for digital processing. Inherent problems from the sensor, such as noise and striping, may be processed out (Price, 1981). Those images not available on digital tape are available in standard film and paper print products. Night-acquired band 8 data are available only as film and prints.

Because the output from the thermal sensor progressively worsened, data acquired during the initial 4-month period of operation (March-July, 1978) are considered optimum. Table 2 lists data acquired by Landsat 3 band 8 during the day. Of the 374 Landsat 3 band 8 images acquired during the day, two were rated good quality (8), 349 were rated fair quality (5), and 23 were rated poor quality (2). Geographic searches were conducted on the INORAC system only for band 8 night coverage over the eastern and western U.S., so the 50+ accessions is not comprehensive. Of the 50+ scenes, all were rated good quality (5). Figure 1 shows sample Landsat 3 band 8 images acquired during day and night passes. Night-acquired band 8 images are skewed opposite daylight images because of the ascending orbit and the direction of Earth rotation. Annotation blocks appear inverted on the northern margin as opposed to the standard Landsat product because the scenes were collected in an opposite sequence.

HCMM

The Heat Capacity Mapping Mission acquired day-visible, day-infrared, and night-infrared data, which are used to generate thermal inertia models of the Earth's surface materials. Some objectives of the mission and recent accomplishments by HCMM investigators include the discrimination of geologic rock units, delineation of lineaments relating to basement structure, and detection possible surface seepage of hydrocarbons trapped at depth (Watson and others, 1981).

Characteristics of the HCMR sensor are listed in table 3. The day-visible image records electromagnetic radiation at wavelengths from the visible into the near IR region (0.55- to 1.1- μ m), which is reflected solar energy. The thermal infrared images record energy emitted from the Earth's surficial materials. The spatial resolution of the visible and IR data are 500 m and 600 m at nadir, respectively. The thermal resolutions of the day- and night-IR data are 2.1^o K and 1.5^o K, respectively.

The HCMR acquired visible and thermal IR data during the day on an ascending orbit (SE to NW) which crossed latitude 40^oN at approximately 1:30 p.m. local time. Thermal IR data were acquired at night on a descending orbit (NE to SW) which crossed latitude 40^o N at approximately 2:30 a.m. local time. This orbit allowed survey of the surface of the Earth near the maximum and minimum of the diurnal cycle providing maximum difference in radiant temperature. From the day-visible, day-infrared, and night-infrared data, temperature difference and thermal inertia data may be derived. Temperature difference is determined by subtracting the radiant temperatures observed by HCMM during the night from those observed during the day. Thermal inertia is computed from the registration of day-visible, day-infrared, and night-infrared images using an algorithm (Price, 1980; Watson and others, 1982). The algorithm, defined by Price (1980), equates the apparent thermal inertia (ATI) to the quotient of the product of the integer

scaling factor (NC) and the quantity $1 - \text{albedo (a)}$ and temperature difference (ΔT) that is $ATI = NC(1-a)/(\Delta T)$. The repeat cycle for day and night orbits occurred at 16-day intervals, however, mid-latitudes were covered approximately every 5 days due to scene overlap. Areas between 22° and 33° , north and south latitude, have a 36-hour interval between day and night coverage. No tape recorders were on board the satellite so receiving station locations restricted coverage to Alaska, conterminous United States, southern Canada, Caribbean, western Europe, north Africa, and east Australia.

HCMM data are archived and distributed by NASA Goddard's National Space Science Data Center (NSSDC) World Data Center - A (WDC - A). Table 4 lists standard image, CCT products, and HCMM information sources. Standard and derivative HCMM data products are presented in figure 2. Approximately 37,628 standard image products, and over 2,500 CCT's and 115 registered day/night scene images and CCT's, have been produced and are available to the public. Image data are catalogued by geographic coordinates on microfiche indexes contained in the HCMM Data User's Handbook. Index maps depicting available HCMM day, night and registered scenes as image and CCT data, have been produced by NASA Goddard (figure 3) and are also available as listings by geographic coordinates. HCMM image products cover an area 700 km by 700 km at a nominal scale of 1:4,000,000 and are the equivalent to the coverage of 16 Landsat images.

The NASA/Goddard image processing facility applies radiometric and geometric corrections, presenting HCMM data in a Hotine Oblique Mercator (HOM) projection (Price, 1980). Prior to the generation of the image from the digital data, linear contrast stretching, from 0-225 values is performed. The image is displayed in gray levels representing 16 equal intervals of digital numbers. The digital numbers are converted to radiant temperatures using a look-up table (Price, 1980). The HCMM images permit qualitative interpretation based on tonal

variations of the gray scale distribution (black, cold; white, hot). As with Landsat MSS data, digital data are required for quantitative analysis. Although spatial resolution is limited and masks features, the small-scale coverage allows regional analysis not provided by current airborne thermal infrared scanners.

'Manual' Interpretation of Landsat 3

Infrared Data

Landsat 3 thermal infrared images were assembled to assess the value and quality of these data for geologic applications. Several data examples covering the western U.S. are manually interpreted and compared with MSS band 7 data.

MSS band 7 (0.8- to 1.1- μm) and band 8 (10.4- to 12.6- μm) of Landsat 3 image E-30087-17240, acquired May 31, 1978, at approximately 10:24 a.m. m.s.t., of the Wind River Range, Wyoming, are presented in figure 4. The Wind River Range, located in west-central Wyoming, is an anticlinal structure composed of a highly fractured crystalline granite core of Precambrian age. In the band 7 image, the snow-covered mountain range is overlain by scattered cumulus clouds. The reflectance of snow and clouds impede identification of surface features because brightness saturates the sensor. Band 8 thermal data provide tonal variations within the snow cover suggesting topographic variation and geologic structure.

Temperature anomalies associated with elevation differences and evaporative cooling of deep snow and water concentrated along major fractures are observed in the thermal data although they are masked out in the band 7 reflective solar data. The differentiation between snow and clouds, which have similar spectral reflectance in the visible and near-infrared, is provided in the thermal data in which clouds produce a cool (dark) signature. This tonal anomaly could be used to distinguish clouds and snow in areas such as the polar regions.

Hydrologic features with similar reflectance values in band 7, such as deep glacial lakes and shallow basin lakes, can be differentiated by temperature variations of the water. Daytime thermal imagery provides information on topographic relief in areas with high reflectance (Lougeay, 1982).

Landsat 3 MSS bands 7 and 8, E-30087-17260 acquired May 31, 1978, at 10:26 a.m. m.s.t., and Landsat 3 MSS band 8 data, E-30065-04292 acquired May 9, 1978, at 2:29 a.m. m.s.t., over the Grand Canyon, north-central Arizona, are presented in figure 5.

The Kaibab Plateau (1), a national forest densely vegetated with juniper, pine, and Douglas fir, provides a dark spectral response in all three images. The dark signature on the band 8 data results from the composite emissivity of the conifer needle cluster which approaches that of a black body (Sabins, 1978). In contrast, the non-vegetated sedimentary rocks of Precambrian through Permian age, which compose the steep canyon walls, display a high thermal inertia in both day- and night-IR images and appear bright. Heat trapped and reradiated from canyon wall to canyon wall produces a high thermal inertia at night and contributes to the high thermal inertia (brightness) displayed by the Colorado River area. Topographic features, such as Echo Cliffs (2), Moenkopi (3) and Coconino Plateaus (4), and the San Francisco Mountains (5), are distinguished by tonal variations on the thermal data which result from differences in elevation, surface cover and composition. Lithologic variations between the San Francisco Volcanic Field of Tertiary and Quaternary Age and surrounding sedimentary units of Pennsylvania, Cretaceous, and Tertiary Age are observed on the image and can be mapped (Wilson and others, 1969). The Sunset Crater lava flow (6), in the volcanic field, displays the highest thermal inertia at night because of its composition and degree of weathering in relation to the other flows.

Digital Analysis of HCMM Data

The small scale and regional coverage provided by HCMM data prompted the USGS to investigate the use of these data for the production of large area mosaics (Carter, 1982). HCMM day-visible and day-infrared images (figure 6), AA0546-20060 1/2 acquired 24 October 1979 over the western U.S., were obtained as 9-track 1,600-bpi computer-compatible tapes from NASA/Goddard's NSSDC. Computer processing of the HCMM data was performed July 1981, by Pat Chavez, Jr., USGS, Flagstaff, Arizona.

The raw data were contrast stretched to redistribute the gray-scale density. A 101 by 101 pixel high-pass filter was applied to the HCMM day-visible and day-IR data (figure 7). A high-pass filter (HPF) enhances high frequencies which are represented by rapid changes in brightness over several pixels. Regional lineaments less than half the size of the 101 by 101 pixel box were enhanced by applying a laplacian, or BOXCAR spatial filter (Chavez and others, 1976). Linear features less than 25 to 30 km were enhanced and lineaments more than half the 101-pixel window were suppressed. In comparison with positive film standard product data of the same date, the 101 by 101 HPF produced no significant results.

A band ratio using day-visible (.5-1.1 μm) and day thermal infrared (10.5-12.5 μm) data (figure 8) was then tested. Band ratioing is a technique in which two data sets are spatially registered, divided pixel by pixel and rescaled by contrast stretching. Band ratioing suppresses brightness variations due to topographic relief and enhances subtle spectral variations. Band ratioing also enhances atmospheric affects and noise which are problematic to the interpreter. Wind streaks trending NE across south-central Arizona create tonal anomalies in day-thermal data and the ratio image. Major variations in the reflected versus emitted energy are accentuated by the ratio technique and are displayed by a low value (dark). These include the snow-covered Sierra Nevadas (1), San Francisco Peak (2), Kabito and Moenkopi Plateaus (3), and Danby dry lake (4).

The last technique applied was a diagonal derivative (figure 9). Derivative techniques are designed to enhance the structural fabric of a region. In contrast to the HPF, the derivative procedure highlights brightness differences that occur at a pixel to pixel scale (Chavez and others, 1976), in this case, 500-600 m. The diagonal derivative suppresses lineaments that are diagonal to HCMR scan lines, while highlighting all other linear directions. The diagonal derivative performed on the day-visible data enhances major structural and topographic features which include the San Andreas (1) and Garlock Fault Systems (2), block faulting in the Basin and Range Province (3), and drainage features of Lake Meade (4), Grand Canyon (5), and the Colorado (6) and Gila Rivers (7). The diagonal derivative performed on the day-thermal IR data provides enhanced interpretation of structure and topographic features due to the range and contrast of thermal values. The thermal values of mountain ranges (8) having mafic and felsic composition are distinct from those of basins and pediments (9) composed of unconsolidated gravel, sand, and silt. Thermal anomalies relating to composition of materials or fault controlled groundwater anomalies, are easily identifiable on the thermal diagonal derivative. Atmospheric affects, such as wind streaks in the bottom right corner of the image (10), are also enhanced.

Landsat 4

On July 16, 1982, Landsat 4 carrying an MSS and TM sensor was launched into a nominal 705-km Sun-synchronous polar orbit. The 4-band MSS system is identical, in spectral and spatial resolution, to those carried on Landsat's 1, 2, and 3, with the exception of the thermal band on Landsat 3. The TM sensor consists of 6 narrow spectral bands, recording reflected solar energy with an increased pixel resolution of 30 meter by 30 meter as opposed to the 79-meter MSS. The TM band 6 consists of 4 mercury-cadmium-telluride detectors operating in the 10.4- to 12.5 μm wavelength region. The TM band 6 will produce thermal data with 120-m by 120-m spectral resolution and a radiometric resolution anticipated at 0.5° K noise equivalent temperature difference (NE Δ T). The size of the fiber optics is 4 times larger on TM band 6 than bands 1-5 and 7, thus the sampling rate is $\frac{1}{4}$ that of the other bands.

The Landsat 4 will acquire thermal infrared data during the day with an Equatorial crossing time between 9:30-10:00 a.m. local time. Due to the verification of the ground processing at NASA Goddard Space Flight Center, only 1 TM scene is being processed daily. Additional TM acquired data will be stored on tape for future processing. It is anticipated that by April 1984, 2 scenes will be processed per day with 10 scenes processed daily by January 1985. Landsat 4 MSS and TM data will be archived and distributed by the EROS Data Center, Sioux Falls, S.D. Preliminary information on Landsat 4 can be obtained in the Landsat Data User's Notes issue no. 23 July 1982.

Conclusion

Thermal data acquired by Landsat 3 and HCMM are the only high-resolution (0.5 km) satellite thermal IR data available of the Earth. Although the Landsat 3 band 8 sensor malfunctioned and produced no excellent quality data, day-thermal IR and night-thermal IR data do exist for the majority of the conterminous United States. HCMM acquired a large quantity of good to excellent quality day-visible, day-infrared, and night-infrared data of the United States. Investigators are still reporting on significant results. The geoscience community should gain valuable interpretation experience and processing skills from analyzing the existing Landsat 3 and HCMM data to prepare for accurate exploitation of thermal IR data from the TM on Landsat 4.

Manual interpretation of Landsat 3 thermal IR data provides information on topography and surficial materials that is not provided in existing Landsat solar reflectance data. Digital analysis of HCMM visible and thermal IR data provides new techniques for the study and mapping of regional features. The regional coverage also provides an inexpensive data base for large area analysis. Directional derivatives performed on HCMM thermal-IR data enhance structural fabric and thermal anomalies and provide additional dimensions to satellite remote sensing. The same techniques discussed may be applied to the anticipated TM high-resolution thermal IR data and should provide a useful tool for geologic mapping.

References

- Carter, W. D., 1982, A strategy for mineral and energy resource independence: The North American Plate Mosaic Project: in Abstracts of the 24th COSPAR Meeting, Remote Sensing for Mineral Exploration, (17-21 May, 1982), Ottawa, Canada, p. 96.
- Chavez, P. S., Jr., Berlin, G. L., and Acosta, A. V., 1976, Computer processing of Landsat MSS digital data for linear enhancements: Second Annual Pecora Symposium, (25-29 October, 1976), Sioux Falls, South Dakota, p. 235-250.
- Lougeay, R., 1982, Landsat thermal imaging of alpine regions: Photogrammetric Engineering and Remote Sensing, v. 48, no. 2, p. 269-273.
- Price, J. C., 1980, Heat capacity mapping mission (HCMM) Data User's Handbook for Applications Explorer Mission-A (AEM): Goddard Space Flight Center, NASA, 120 p.
- Price, J. C., 1981, The contributions of thermal data in Landsat multispectral classification: Photogrammetric Engineering and Remote Sensing, v. 47, no. 2, p. 229-236.
- Sabins, F. F., Jr., 1978, Remote sensing, principles and techniques: W. H. Freeman and Company, San Francisco, California, 426 p.
- U.S. Geological Survey, 1979, Landsat data user's handbook, revised edition.
- U.S. Geological Survey, 1982, Landsat data user's notes, issue 23, July 1982.

Watson, K., Hummer-Miller, S., and Offield, T. W., 1981, Geologic applications of thermal-inertia mapping from satellite: Final report - HCMM investigation S-40256-B, prepared for NASA Goddard, 72 p.

Watson, K., Hummer-Miller, S., and Sawatzky, D. L., 1982, Registration of heat capacity mapping mission day and night images: Photogrammetric Engineering and Remote Sensing, v. 48, no. 2, p. 263-268.

Wilson, E. D., Moore, R. T., and Cooper, J. R., 1969, Geologic map of Arizona, 1:500,000-scale, Arizona Bureau of Mines, and U.S. Geological Survey.

LIST OF ILLUSTRATIONS

Figure 1.—(A) Landsat 3 MSS band 8 image (E-30107-17351) acquired June 20, 1978, at approximately 10:35 a.m. m.s.t. over the West Yellowstone, Montana, Wyoming, and Idaho Junction (path 42, row 29). (B) Landsat 3 MSS band 8 image (E-30045-04195) acquired April 19, 1978, at approximately 2:19 a.m. m.s.t. over Idaho Falls, Idaho (path 47, row 30).

Figure 2.—Subscenes of HCMM images acquired on September 26, 1978, over the Appalachian Mountains of Central Pennsylvania. The day visible (A) and the day infrared (B) images were acquired at approximately 1330 hr (e.s.t.); the night infrared (C) image was acquired at approximately 0230 hr (e.s.t.) on the same day. Temperature difference (T) (D) was produced by subtracting the radiometric temperatures observed by the HCMM during the day and night passes. Thermal inertia (E) is a derivative product of the day and night thermal images (T values). The marked difference in the composition of the surface material of the folded Appalachian strata and the glacial deposits around the Finger Lakes region can be observed. Urban heat islands are observed in both the day and night thermal infrared images as bright spots. The ridges of the Appalachian Mountains, composed of quartzite and dolomite, and regional ground water patterns, display high thermal inertia at night. (Courtesy H. Pohn, USGS).

Figure 3.—Index maps depicting HCMM day (A) and day/night image coverage (B) of a portion of the eastern United States. Products available include film and computer compatible tapes (see table 4). (Map courtesy NASA/Goddard Space Flight Center).

Figure 4.—Landsat 3 MSS band 7 (a) and band 8 (b) images acquired May 31, 1978, at approximately 10:24 a.m. m.s.t. (E-30087-17240), Wind River Range, west central Wyoming (path 40, row 30).

Figure 5.--Landsat 3 MSS band 7 (a) and band 8 (b) images acquired May 31, 1978, at 10:26 a.m. RMT (E-30087-17260), and Landsat 3 MSS band 8 (c) image acquired May 9, 1978, at 2:29 a.m. RMT (E-30065-04292), over the Kaibab Plateau and Grand Canyon, north central Arizona.

Figure 6.--HCMM day visible (a) and day infrared (b) imagery acquired October 24, 1979, (E-AA0546-20060-1/2) over the southwestern U.S. (Standard products courtesy of NASA.)

Figure 7.--101 x 101 high-pass filter applied to HCMM day-visible (a) and day-infrared (b) images of the same date as figure 6. (Processing courtesy P. Chavez, Jr., USGS/IPF, Flagstaff, Ariz.)

Figure 8.--Band ratio of HCMM day visible to day infrared image of October 24, 1979. Band ratio techniques suppress brightness variations due to topographic relief.

Figure 9.--Diagonal derivative applied to HCMM day visible (a) and day infrared (b) images acquired October 24, 1979. Thermal anomalies relating to topographic and compositional variations are enhanced in the day infrared image (b).

TABLE 1

LANDSAT 3 MSS BAND 8 CHARACTERISTICS

Spectral Band	10.4 to 12.6 micrometers
Thermal Detection	260° to 340°K
Instantaneous Field of View	238 x 238 meters (nominal)
Number of Sensors	2
Lines/Mirror Scan	2
Swath Width	100 nm (nautical miles)
Detector Material	Hg Cd Te
NEAT (Noise Equivalent Temperature)	1.4°K for 300°K scene
In-Flight Calibration	(A) Ambient black body (B) Reflected Detectors

(Modified after Landsat Data Users Handbook, 1979, revised edition, U.S. Geological Survey)

Table 2

CHRONOLOGICAL COVERAGE OF LANDSAT 3 MSS BAND 8 DAY-
ACQUIRED IMAGES OF THE CONTERMINOUS UNITED STATES

<u>DATE</u>	<u>PATH(S)</u>
3/26/78	46
3/27/78	47
4/5/78	38
4/9/78	42
4/17/78	14
4/17/78	32, 50
4/18/78	15
4/19/78	34
4/20/78	35
4/24/78	39
4/25/78	40, 22
4/26/78	41, 23
5/3/78	48
5/6/78	15, 33, 51
5/7/78	16
5/8/78	17, 35
5/9/78	18, 36
5/10/78	19, 37
5/12/78	21, 39
5/13/78	22
5/15/78	42
5/16/78	25, 43
5/18/78	27, 45
5/19/78	28, 46
5/25/78	16, 34
5/26/78	35
5/29/78	20, 38
5/30/78	21, 39
5/31/78	22, 40
6/2/78	24
6/3/78	25, 43
6/5/78	27, 45
6/6/78	28, 46
6/7/78	11, 29, 47
6/19/78	41
6/20/78	24, 42
6/21/78	25, 43
6/22/78	26
6/23/78	27
6/25/78	11, 29, 47
6/26/78	12, 48
6/27/78	13, 49
6/28/78	14
6/30/78	16, 34

Table 3

Characteristics of Heat Capacity Mapping Radiometer (HCMR)

	IFOV (Instantaneous Swath field of view) width				NER/NE Δ T (Noise equivalent radiance/Noise equivalent temperature difference)
	<u>Wavelength</u>	<u>field of view)</u>	<u>width</u>	<u>Range</u>	<u>equivalent temperature difference</u>
Visible channel,	0.55-1.1 μ m	500 m	716 km	0-100% Albedo	0.2 milliwatt/centimeter ² (NER)
Thermal channel,	10.5-12.5 μ m	600 m	716 km	260 ^o K-340 ^o K	0.3 ^o K at 280 ^o K (system NE Δ T; 0.4 ^o K at 280 ^o K)

Table 4
HCMM DATA

<u>STANDARD PRODUCTS</u>	<u>INFORMATION</u>
1:4,000,000-scale images on 241-mm film or print, black and white (positive or negative):	National Space Science Data Center/World Data Center-A Code 601
Day visible.	NASA/GSFC
Day infrared.	Greenbelt, MD 20771
Night infrared.	(301) 344-6695
Temperature Difference, (Night vs. day).	HCMM Data Users Handbook and HCMM Data Users Bulletin
Thermal Inertia.	Code 902
Computer compatible tapes	NASA/GSFC
9-track, 800 and 1600-bpi	Greenbelt, MD 20771 (301) 344-5770

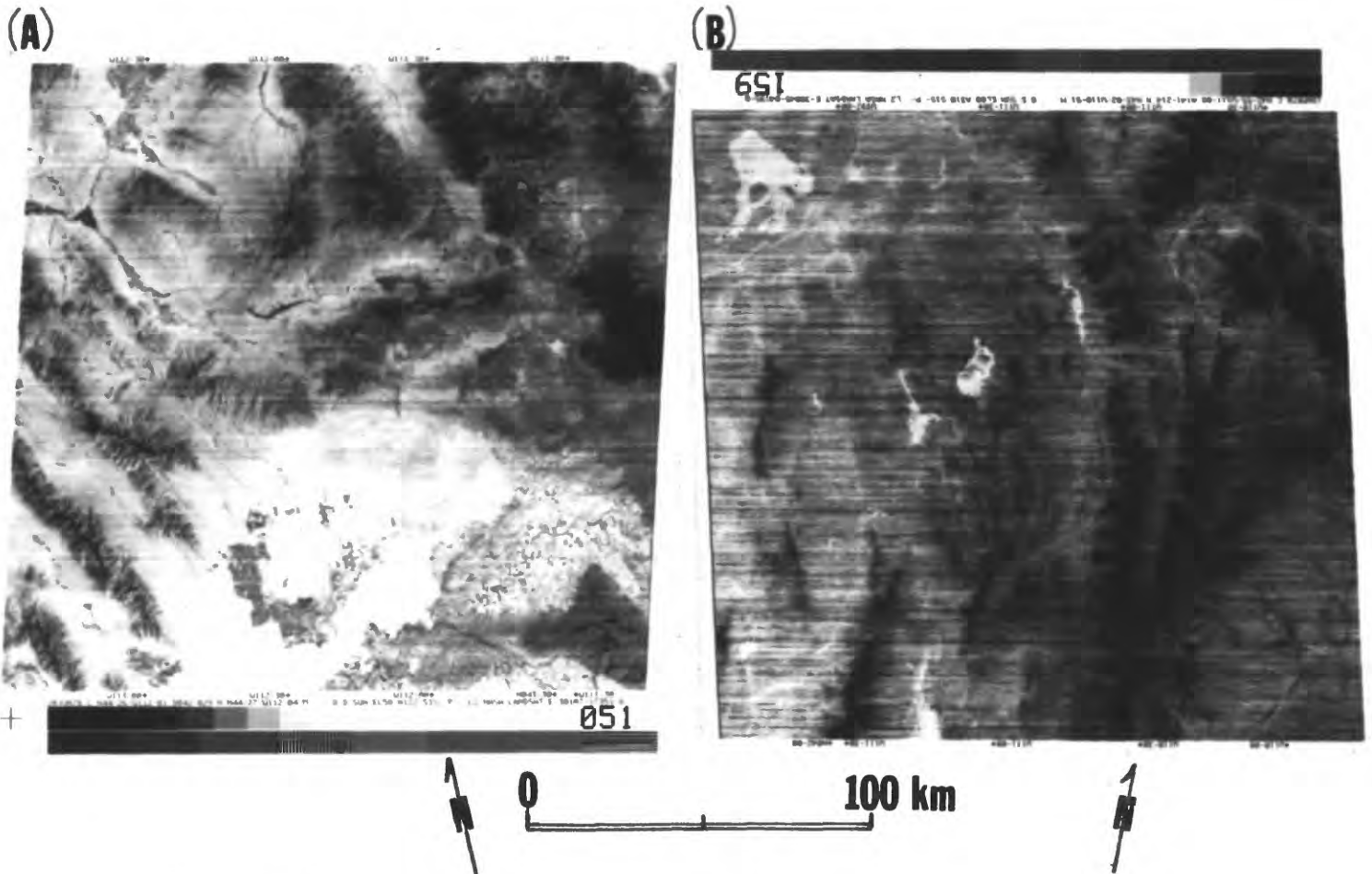


Figure 1.--(A) Landsat 3 MSS band 8 image (E-30107-17351) acquired June 20, 1978, at approximately 10:35 a.m. m.s.t. over the West Yellowstone, Montana, Wyoming, and Idaho Junction (path 42, row 29). (B) Landsat 3 MSS band 8 image (E-30045-04195) acquired April 19, 1978, at approximately 2:19 a.m. m.s.t. over Idaho Falls, Idaho (path 47, row 30).

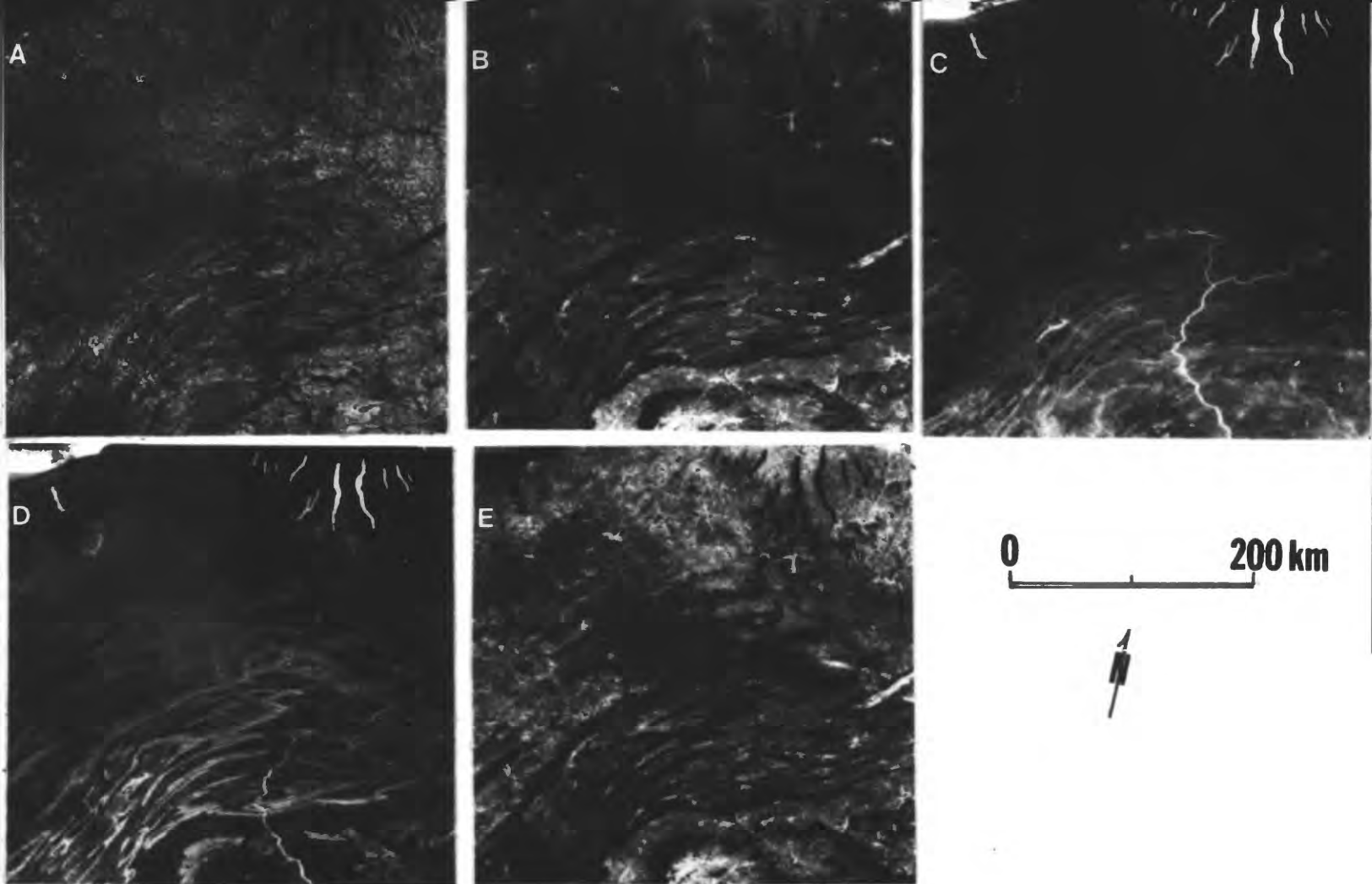


Figure 2.--Subscenes of HCMM images acquired on September 26, 1978, over the Appalachian Mountains of Central Pennsylvania. The day visible (A) and the day infrared (B) images were acquired at approximately 1:30 p.m. (e.s.t.); the night infrared (C) images was acquired at approximately 2:30 a.m. (e.s.t.) on the same day. Temperature difference (ΔT) (D) was produced by subtracting the radiometric temperatures observed by the HCMM during the day and night passes. Thermal inertia (E) is a derivative product of the day and night thermal images (T values). The marked difference in the composition of the surface material of the folded Appalachian strata and the glacial deposits around the Finger Lakes region can be observed. Urban heat islands are observed in both the day and night thermal infrared images as bright spots. The ridges of the Appalachian Mountains, composed of quartzite and dolomite, and regional ground water patterns, display high thermal inertia at night (Courtesy H. Pohn, USGS).

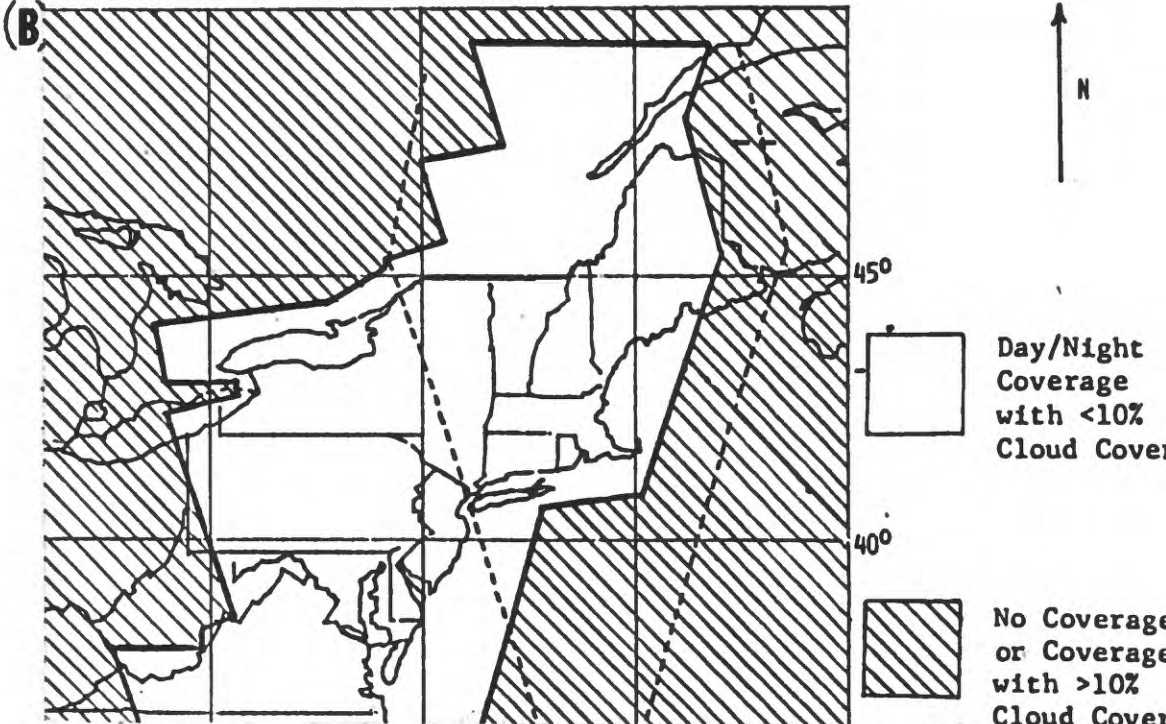
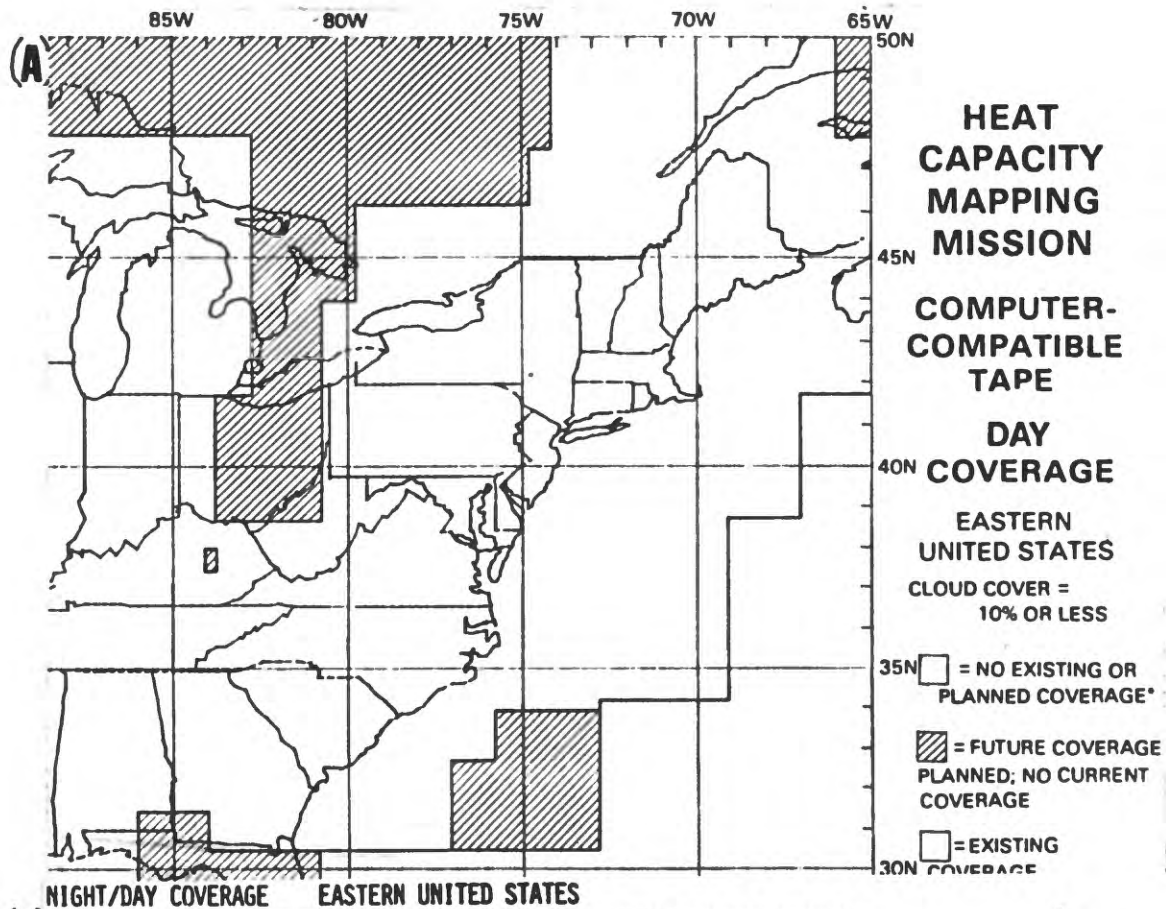


Figure 3.--Index maps depicting HCMM day (A) and day/night image coverage (B)

of a portion of the eastern United States. Products available include film and computer compatible tapes (see table 4) (map courtesy NASA/Goddard Space Flight Center).

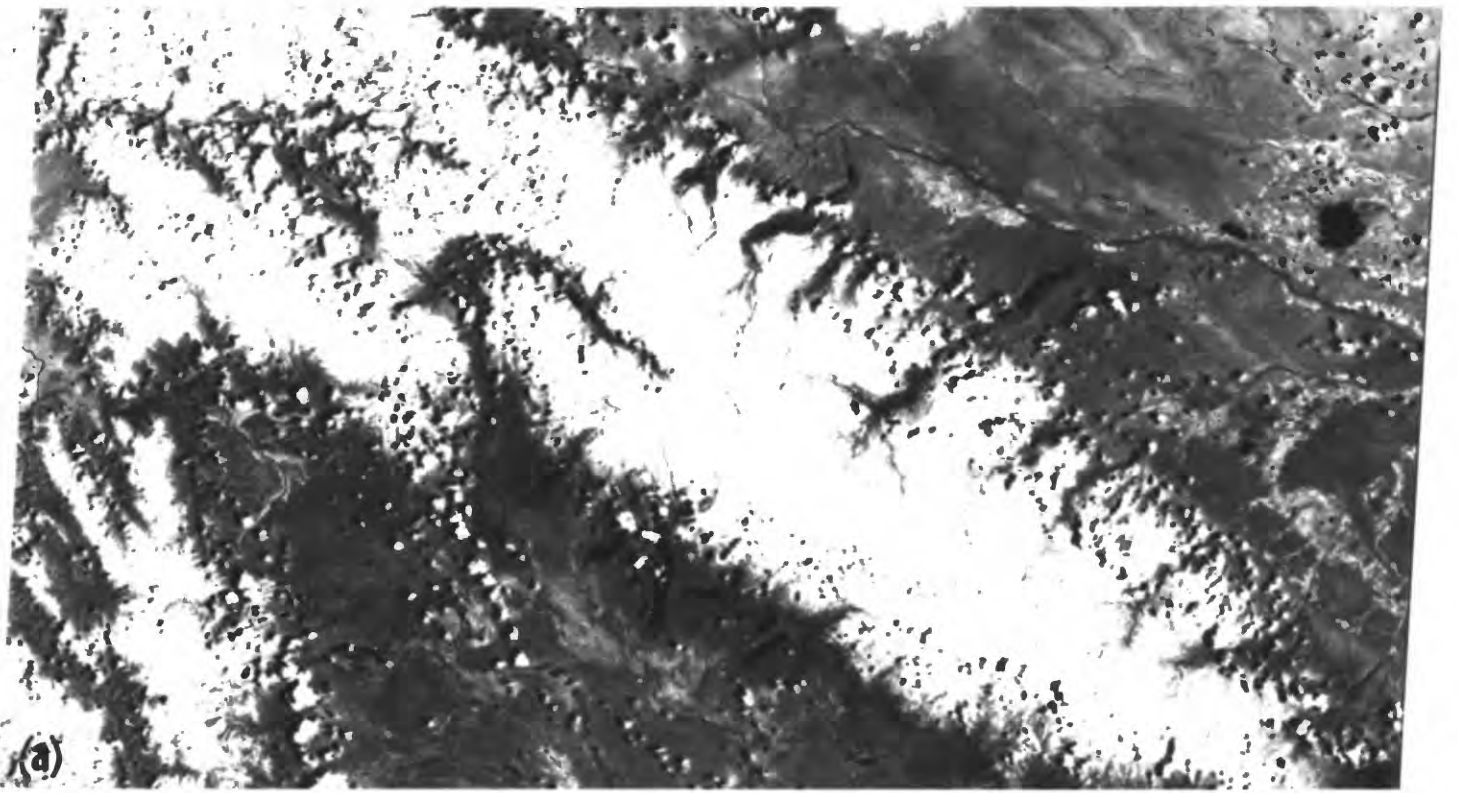


Figure 4.--Portions of Landsat 3 MSS band 7 (a) and band 8 (b) images acquired May 31, 1978, at approximately 10:24 a.m. m.s.t. (E-30087-17240), Wind River Range, west-central Wyoming (path 40, row 30).

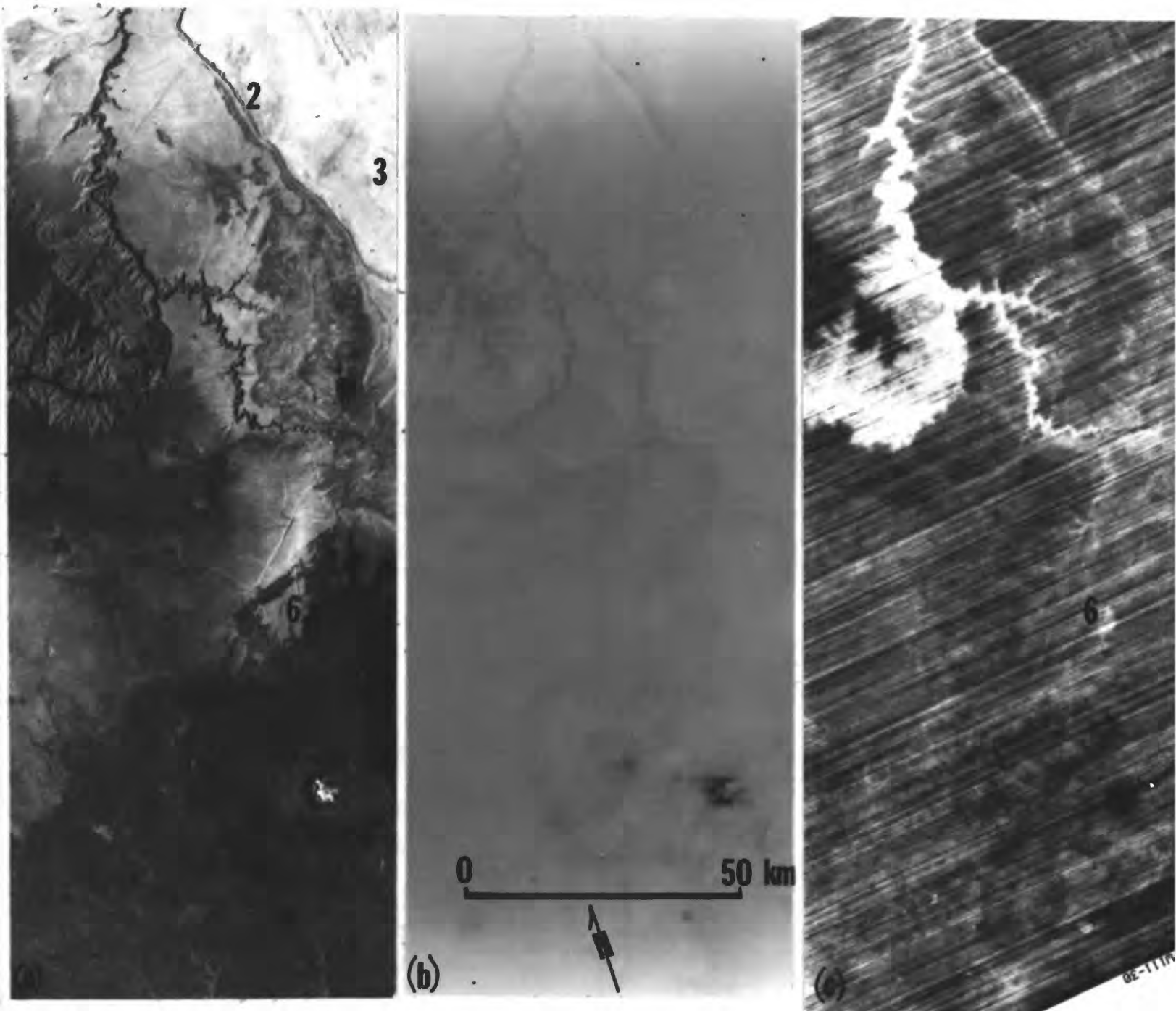


Figure 5.--Portion of Landsat 3 MSS band 7 (a) and band 8 (b) images acquired May 31, 1978, at 10:26 a.m. m.s.t. (E-30087-17260), and Landsat 3 MSS band 8 (c) image acquired May 9, 1978, at 2:29 a.m. m.s.t. (E-30065-04292), over the Kaibab Plateau and Grand Canyon, north-central Arizona.

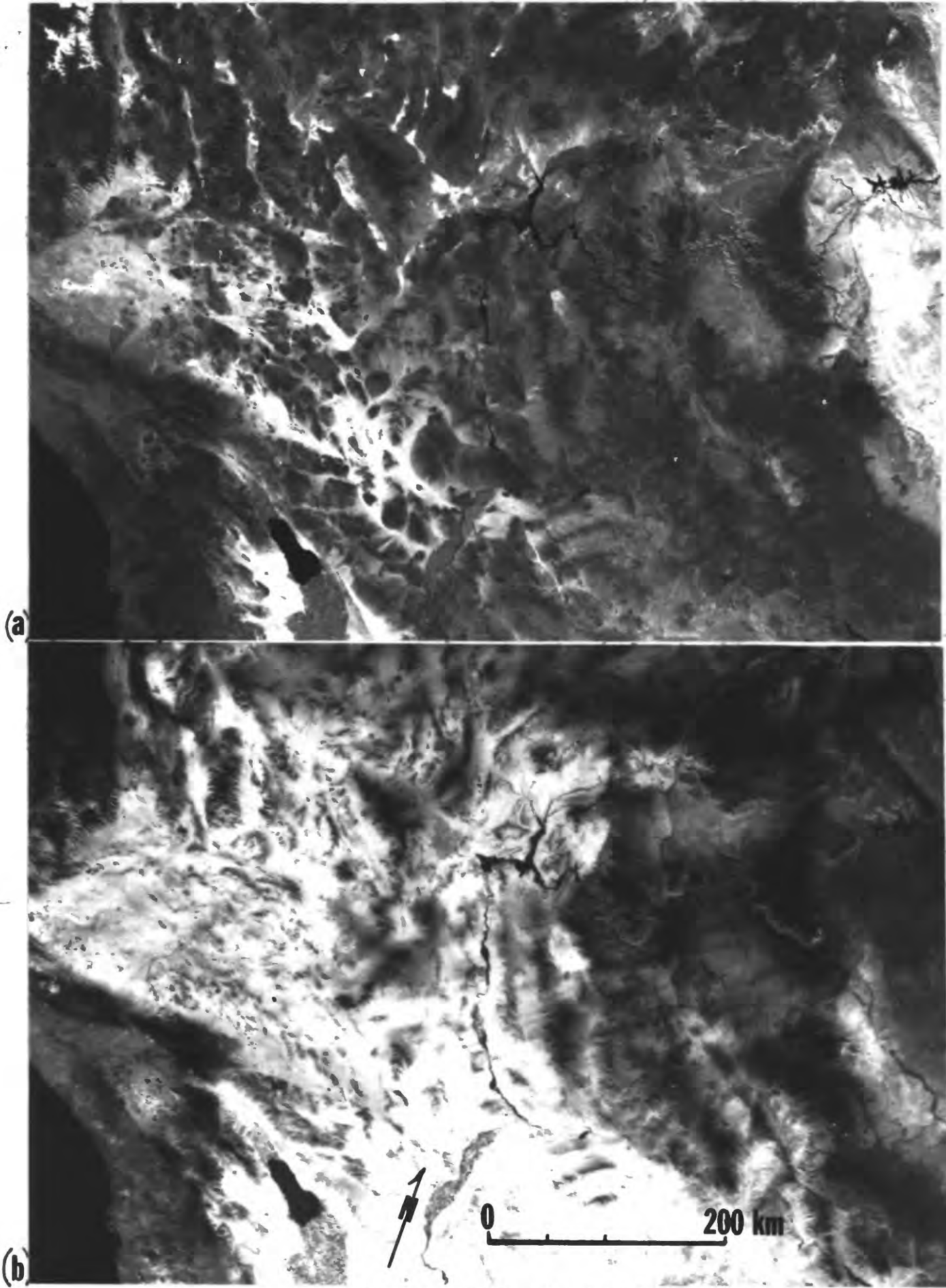


Figure 6.--Portion of a HCMM day visible (a) and day infrared (b) imagery acquired October 24, 1979, (AA0546-20060-1/2) over the southwestern U.S. (Standard products courtesy of NASA).

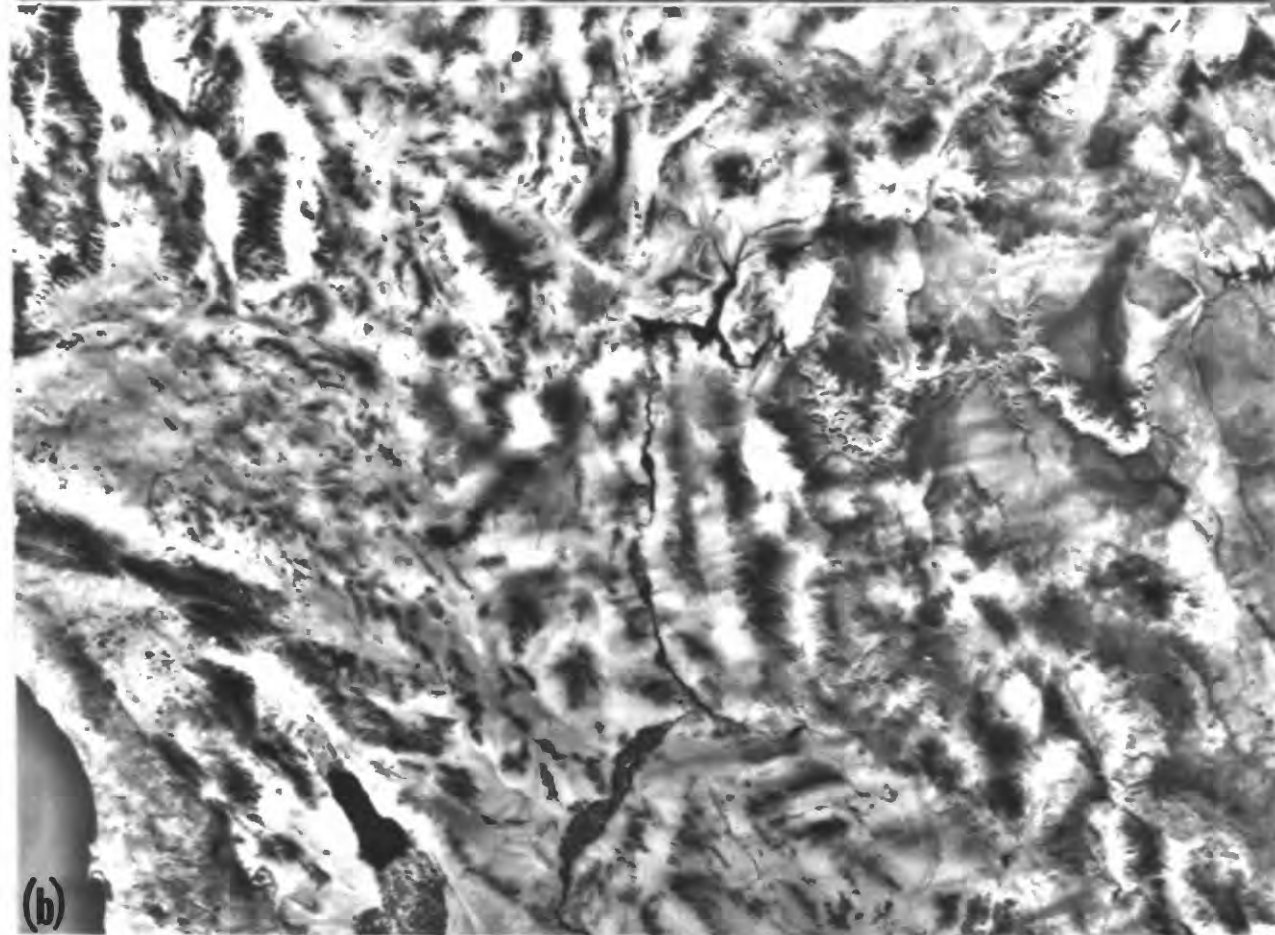
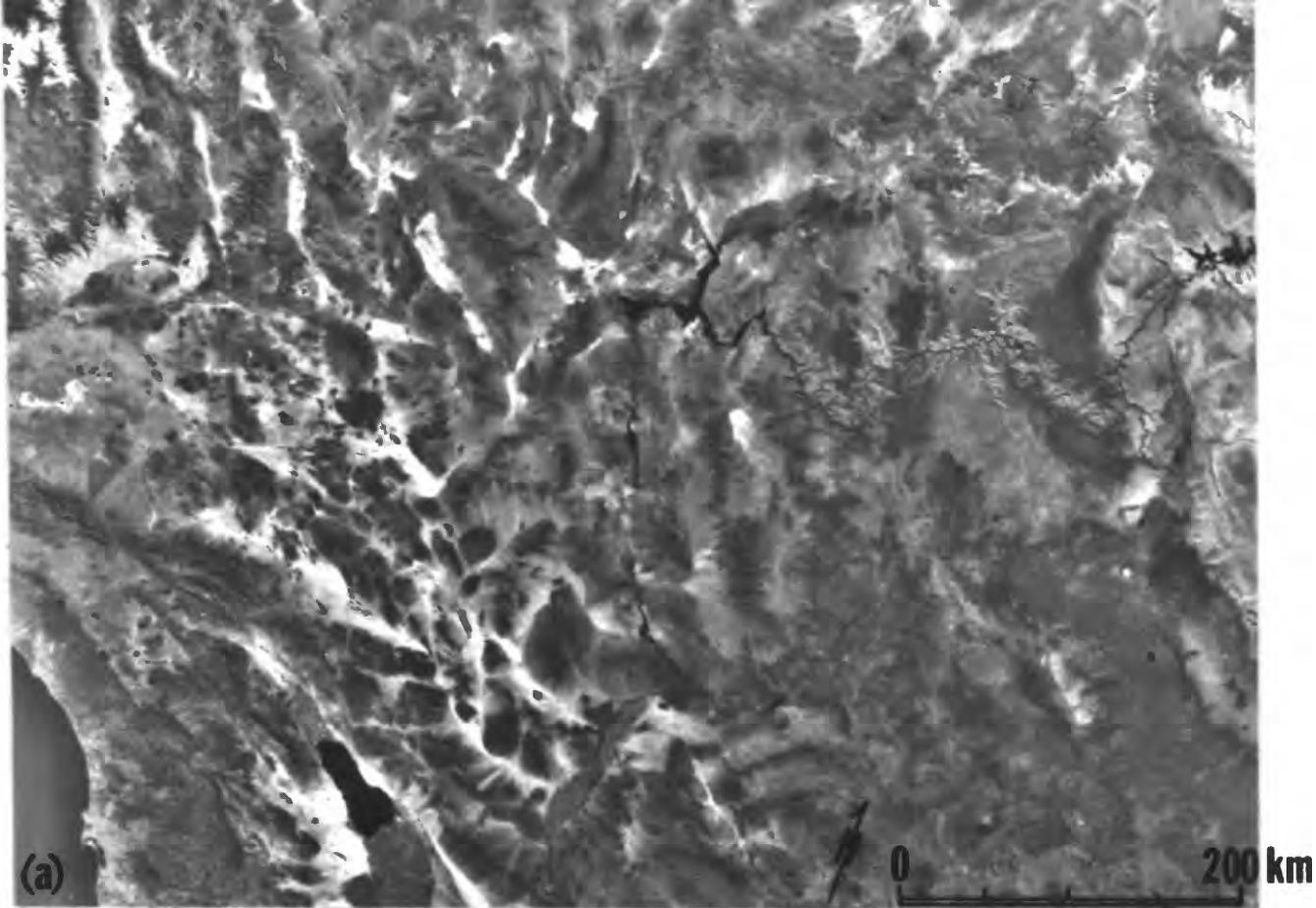


Figure 7.--101 x 101 pixel high pass filter applied to HCMM day visible (a) and day infrared (b) images of the same date as figure 6. (Processing by P. Chavez, Jr., USGS/IPF, Flagstaff, Arizona).

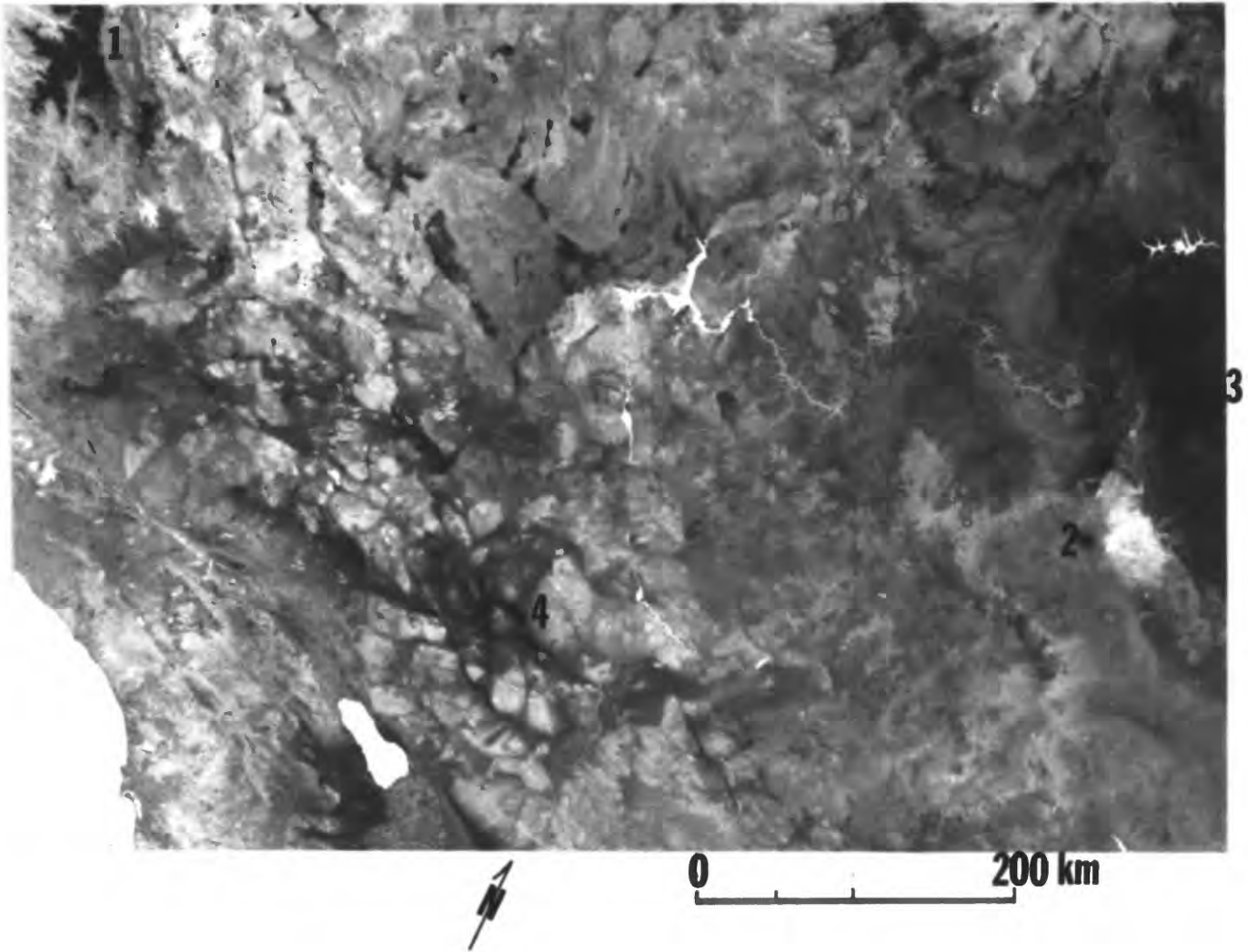


Figure 8.--Band ratio of HCMM day visible to day infrared images of October 24, 1979. Band ratio techniques suppress brightness variations due to topographic relief.

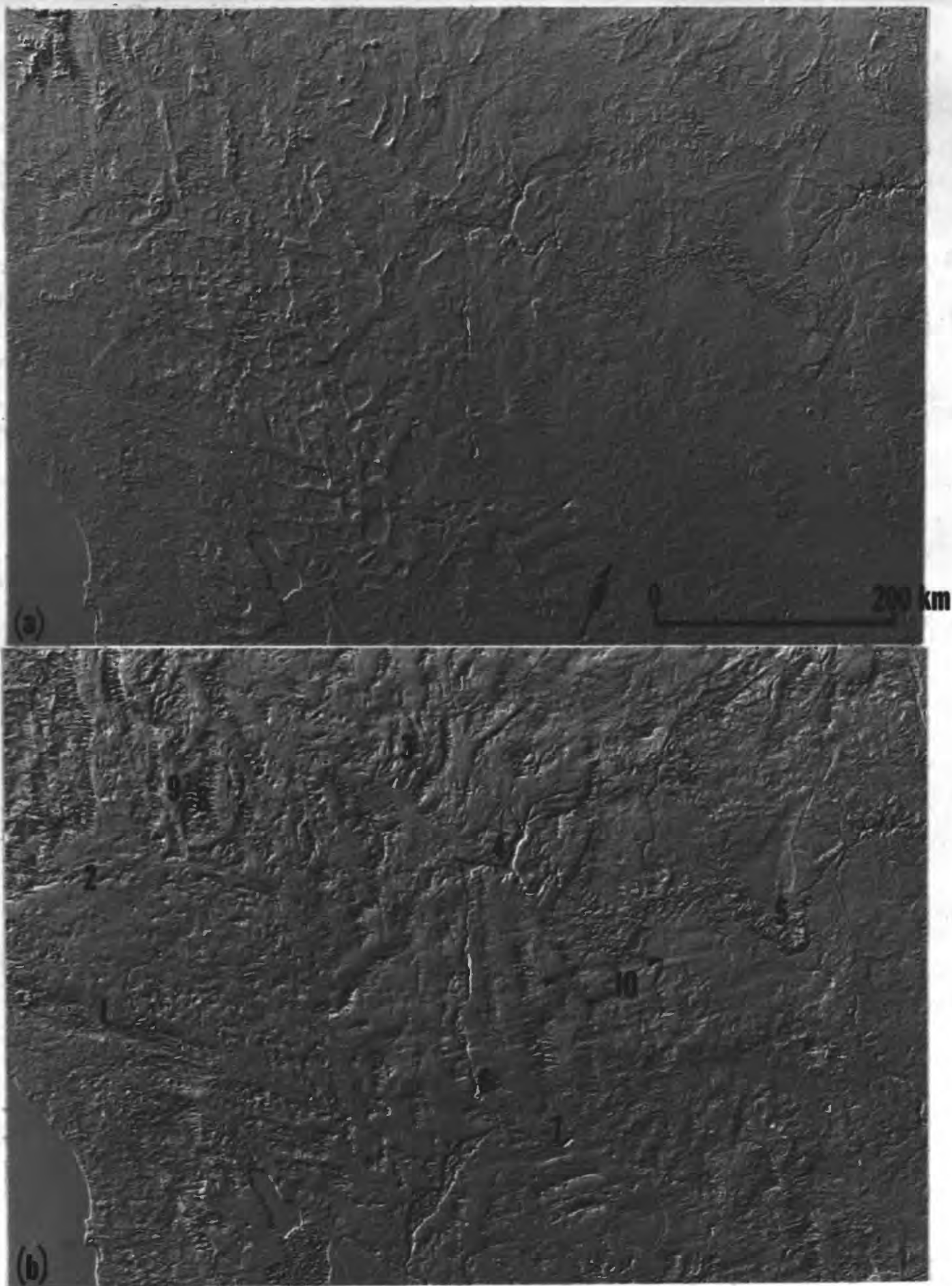


Figure 9.--Diagonal derivative applied to HCMM day visible (a) and day infrared (b) images acquired October 24, 1979. Thermal anomalies relating to topographic and compositional variations are enhanced in the day infrared image (b).